

Supplemental Material for “Revealing dynamics, communities, and criticality from data”

Deniz Eroglu^{1,2,3,*}, Matteo Tanzi^{2,4}, Sebastian van Strien², and Tiago Pereira^{1,2}
¹*Instituto de Ciências Matemáticas e Computação, Universidade de São Paulo, São Carlos, Brazil*
²*Department of Mathematics, Imperial College London, London, UK*
³*Department of Bioinformatics and Genetics, Kadir Has University, 34083 Istanbul, Turkey and*
⁴*Department of Mathematics and Statistics, University of Victoria, Victoria BC, CA*

I. COMPARISON WITH THE SPARSE RECOVERY

This method gives a way of recovering the equations from data by considering the evolution map as a linear combination of a well chosen basis of functions, called library. The main assumption is that many coefficients will be zero. That is, the vector of coefficients will be sparse [1], and some of the nonzero coefficients can give, in many cases, information on the network structure. However, this method does not work in our case where interactions are very small, and coefficients identifying the presence of a link are very close to zero. Since we have N nodes in our network, we consider the library $\mathcal{L} = [\phi_1(x_1), \phi_1(x_2), \dots, \phi_1(x_N), \phi_2(x_1, x_N), \dots, \phi_k(x_N, x_N)]$ as the set of basis functions. And denote matrix X and concatenating the vectors $(x_i(t_2), \dots, x_i(t_n))^*$ for $i = 1, \dots, N$ respectively, where $*$ denotes the transpose and we introduce

$$\Theta = \begin{pmatrix} \phi_1(x_1(t_1)) & \dots & \phi_k(x_N(t_1), x_N(t_1)) \\ \phi_1(x_1(t_2)) & \dots & \phi_k(x_N(t_2), x_N(t_2)) \\ \vdots & \vdots & \vdots \\ \phi_1(x_1(t_{n-1})) & \dots & \phi_k(x_N(t_{n-1}), x_N(t_{n-1})) \end{pmatrix}$$

We then look for a solution of the system $X = \Theta \Xi$ where Ξ is the matrix of coefficients. The sparse recovery technique then solves the linear equation for Ξ iteratively enforcing the sparsity of Ξ by introducing σ such that if $|\zeta_{ij}| \leq \sigma$ we set such entry to zero [1].

In our case, we have considered the scenario where the synopsis between neurons are electric and we generate the multivariate data for the cat cerebral cortex. We assumed we have knowledge of the coupling function so we can easily read the network structure from the sparse recovery. We choose a library of polynomials as $\phi_j(x_i) = x_i^j$ for $j = \{1, \dots, 5\}$ and the pairwise $\phi_j(x_i, x_k)$ to be homogeneous polynomials of degree two in the variables x_i and x_k for $i, k \in \{1, \dots, N\}$.

II. RECONSTRUCTION OF DEGREE DISTRIBUTIONS

Scale-free networks. We create ensembles of scale-free network of $N = 6000$ nodes with distinct structural exponents γ following the same technique as in the main body of the manuscript. As in the main body, we only consider the largest connected component of the network (giant component). For each network realisation we compute the largest

degree Δ and, for simplicity, we fix the coupling strength $\alpha/\Delta = 0.5$ throughout the rest of the section.

A. Doubling map

Let us now apply our approach when F_i is a perturbed version of the doubling map. Since the dynamics is one dimensional, we denote $x = x$ and $F_i(x) = f_i(x)$ with

$$f_i(x) = 2x + \varepsilon_i \sin 2\pi x \mod 1$$

and where we take ε_i to be i.i.d. random variables (i.e. independent over i) uniformly distributed on $[0, 10^{-3}]$. Likewise we write $H = h$ with

$$h(x_j, x_i) = \sin 2\pi x_j - \sin 2\pi x_i.$$

We fixed $\alpha = 10^{-2}$. Since the unique absolutely continuous invariant measure for the doubling map is the Lebesgue measure m , we have

$$V(x) = v(x) = \int h(y, x) dm(y)$$

yielding $v(x) = -\sin 2\pi x$ and the reduced dynamics takes the form

$$x_i(t+1) = f_i(x(t)) - \alpha k_i v(x(t)) + \alpha \xi_i(t).$$

We aim to recover the reduced dynamics and in particular f and v from the data of a multivariate time series with $T = 2000$ time steps.

From data to Model. We assume not to have access to the network structure and only measure the time-series $\{x_i(t)\}$ at each node, as illustrated in Figure 1 Data. By performing the steps described in the main body of the manuscript, we can recover an effective network. We now illustrate in detail our procedure in the case above of the doubling map.

(i) Reduced dynamics. From the time series observed at each node, we construct the attractor for that particular node. Computing the embedding dimension we notice that the dynamic at each site (node) is well described by a one dimensional map, $g_i(x) = f_i(x) - \alpha k_i v(x)$, up to a fluctuation ξ_i . Hence, to reconstruct the attractor it suffices to obtain the return map. Return maps at different nodes are shown in Figure 1 (i).

(ii) Isolated dynamics and effective coupling. We start by introducing a similarity measure.

* deniz.eroglu@khas.edu.tr

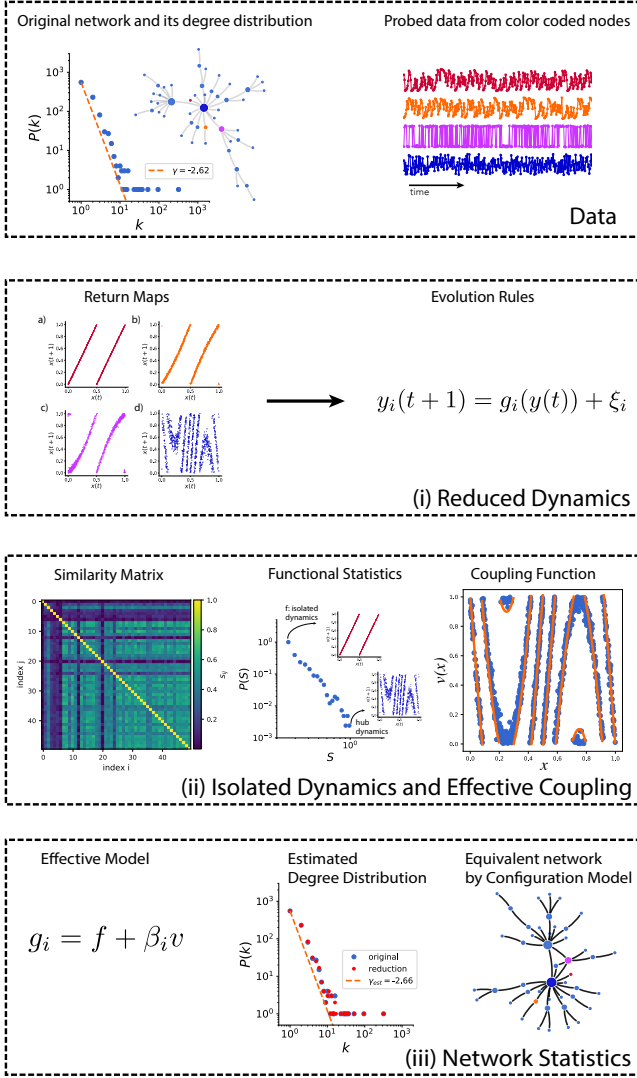


FIG. 1. Step-by-step construction of an effective network for doubling maps coupled on a scale free network. Our approach recovers the local dynamics of the doubling map, interaction function and statistical structure from the time series. Starting from datasets we uncover the approximate evolution rule for the time series using machine learning techniques. Such rules will be different for different nodes (depending on their degree) as shown in panel (i). Analysing the differences between these rules by means of a similarity analysis, we are able to obtain model of the isolated dynamics and an estimate the coupling function, see panel (ii). Finally, by using the theory of dynamical systems and dimensional reduction, we are able to estimate the number of input each node receives and the community structures. We then create a random presentation of the network structure by using a network model such as the configuration model.

Similarity of the time series. Two time series are considered almost the same, if whenever $y_i(t)$ and $y_j(t')$ are close then $y_i(t+1)$ and $y_j(t'+1)$ are also close. This means that one considers the new times series $z_i(t) := (y_i(t), y_i(t+1))$, $z_j(t) := (y_j(t), y_j(t+1))$, $t = 0, \dots, T-1$, reshuffle them according to the lexicographical ordering (i.e. according to

the magnitude of the first coordinate), and then take s_{ij} to be the Pearson correlation distance between these reshuffled sequences. So if the time series at i and j are just out of phase, then, thanks to the reordering, their distance $s_{ij} = 0$. We then calculate the intensities $S_i = \sum_j s_{ij}$ and use this to classify the nodes. The similarity matrix is shown in Figure 1(ii).

Using the correlation distance described above, we determine for which nodes S_i is minimal and in this way we identify the low degree nodes. For the low degree nodes, the sequence $\{(y_i(t), y_i(t+1))\}_{t=0, \dots, T-1}$ lies close to the graph of the return map for f , and thus we obtain a good estimate for the isolated dynamics f , see Figure 1(ii). Next, we apply the reduction to estimate the coupling function.

To obtain the effective coupling v from data, take a hub j and consider the sequence $\{(y_j(t), y_j(t+1))\}_{t=1}^{2000}$. The resulting time series approximates the graph of g_i and subtracting f gives an approximation of the function v up to a multiplicative constant (shown in Figure 1(ii)).

(iii) Network Structural Statistics. There are two ways to obtain information about the statistics of the degrees k_i . The first one uses the noise variance. In fact, the size of the fluctuations ξ_i depends on the number of connections the node i makes, and with good approximation $\text{Var}(\xi_i) \propto k_i$. The second one uses f and v recovered at the previous step. For every node i , choose β_i to fit the time series $\{(y_i(t), y_i(t+1))\}_{t=0, \dots, T-1}$ with the map

$$g_i(y) = f(y) - \beta_i v(y).$$

The value of β_i is obtained by Bayesian inference on the return maps is shown in the first panel of Figure 1(i) as f and v . The distribution of β_i will be linear proportional to the degree distribution and so we can use it to obtain the structural parameter. At this point we can construct an effective network with degree distribution close to that of the real network can be constructed with the configuration model as discussed in the main body of the manuscript. We can also check whether there are communities in the network by analyzing the covariance of the fluctuations ξ_i .

In Figure 2 a) we reconstruct from the distribution of β_i the structural exponent γ for 1000 scale-free network with exponents ranging from 2.4 to 3.6

B. Robustness of the reconstruction under noise

Adding some small independent noise to the dynamics does not influence much the reconstruction procedure for the doubling map. This is a consequence of stochastic stability of the local dynamics together with the persistence of the reduction [2]. On the other hand, when the fluctuations become too large the reconstruction will underestimate the network structure. To illustrate these effects, we consider the randomly perturbed doubling maps

$$x_i(t+1) = f_i(x(t)) + \eta_i(t)$$

where the random variables $\eta_i(t)$ are independent over i and t , and identically distributed uniformly in the interval $[-\eta_0, \eta_0]$.

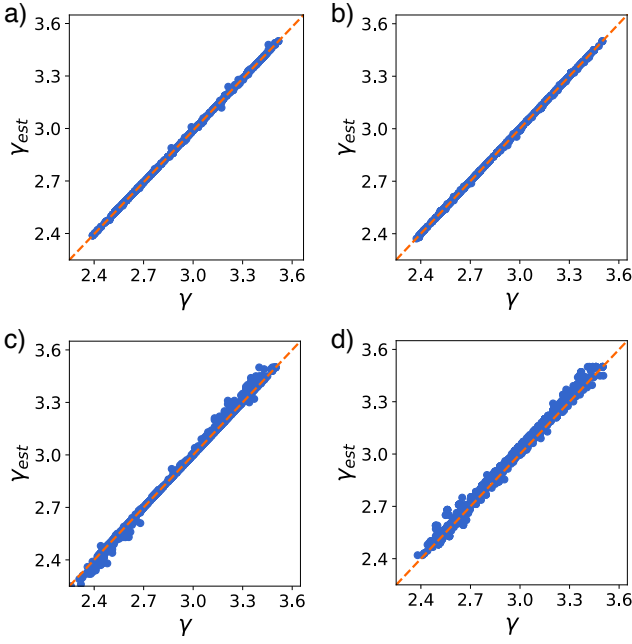


FIG. 2. Recovering the structural parameter of scale free networks using effective networks. The power-law exponent γ versus the estimated γ_{est} from data for 1000 distinct networks. Inset a) shows the reconstruction for coupled doubling maps with diffusive coupling. Inset b) shows the reconstruction for coupled logistic maps with Kuramoto interactions. Inset c) Spiking neurons with electrical coupling, and finally, inset d) shows the reconstruction for the Hénon maps with the y -component diffusive coupled at the x -component.

Intuitively, as long as $\eta_0 < \alpha \min k_i$ the reconstruction will go through as the noise fluctuation will not compete with the coupling term. Notice that we normalize $\|v\| = 1$. This is illustrated in Figure 3. In inset a) the noise has a large support $\varepsilon = 0.1$, and in particular larger than the coupling $\alpha \min k_i = 10^{-2}$. As a consequence, the reconstruction underestimates the number of low degree nodes. In inset b) the noise has a small support $\varepsilon = 10^{-3}$.

C. Coupled Roessler Oscillators

Assume that the local dynamics is modelled by a Rössler oscillator [4]. The dynamics is now in continuous time and our method can also be applied by using a suitable Poincaré section. This gives an induced map that describes the dynamics of the system at specific instants of time (when the system hits a selected subset of phase space). Denoting $\mathbf{x} = (x, y, z)^*$ the vector field is given by $\mathbf{F}(\mathbf{x}) = (y - z, x + 0.2y, 0.2 + z(x - 9))$ and the coupling function, assumed to be diffusive, is given by $\mathbf{H}(\mathbf{x}_i, \mathbf{x}_j) = \mathbf{E}(\mathbf{x}_j - \mathbf{x}_i)$, where \mathbf{E} projects to the first component, i.e., $\mathbf{E}(x, y, z) = (x, 0, 0)$. So, our main equation reads as

$$\dot{\mathbf{x}} = \mathbf{F}(\mathbf{x}) + \alpha \sum_{j=1}^N A_{ij} \mathbf{E}(\mathbf{x}_j - \mathbf{x}_i) \quad (1)$$

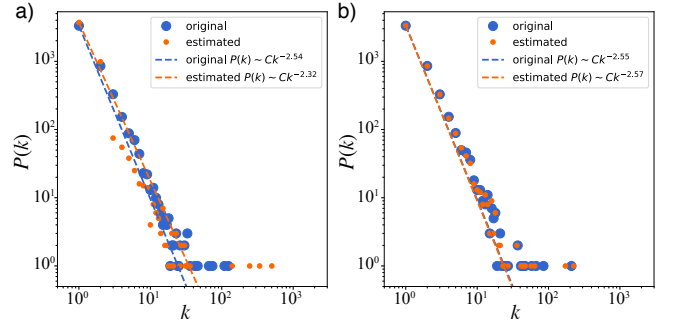


FIG. 3. [Color Online] Effective networks are robust under random perturbations. When stochastic perturbations are moderate effective networks provide sharp estimates on the network structure. If the noise is large, the difference between the time-series at low and high degree nodes becomes blurred. In this case even the effective network underestimates the structural parameter γ . Inset a) shows the reconstruction of the degree distribution for $\varepsilon_0 = 0.1$. Inset b) shows that the reconstruction is unaffected by the noise for $\varepsilon_0 = 10^{-3}$.

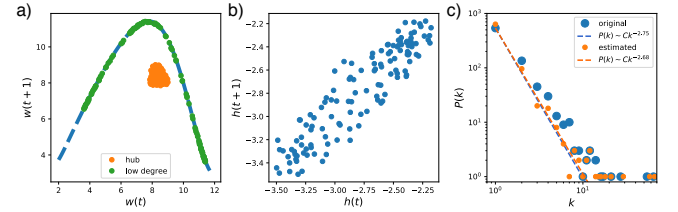


FIG. 4. Main estimations of the reconstruction for the Rössler systems. In inset a) we show the return maps obtained from the time-series of a hub and a low-degree node. Inset b) shows a return plot for the coupling function which is used to estimate the reduced dynamics and the degrees. Inset (c) shows the power-law distribution of the degrees estimated from data and for the original network.

We perform a numerical integration of the equations on the Rich-Club network using a 4th order Runge-Kutta with integration step 10^{-4} and get the data $\{x_i(t)\}_{t \geq 0}$. Using a statistical analysis of the time-series of the state variables, we are not able to reveal the connectivity structure.

The data is phase coherent, that is, taking a Hilbert Transform we can decompose the time series in terms of amplitude and phase we conclude that the spread in the phase variable is small and thus the return time to a given section is nearly constant. So, we consider the Poincaré section defined by the maxima w_i of the time series $x_i(t)$. This gives us a time series $\{w_i(n)\}$ indexing all maxima. We then apply all the steps of the reconstruction procedure to this time series. Because of the coherent dynamics of the phase, the coupling form is preserved in the Poincaré section. The results of the network structure estimation are presented in Figure 4.

III. RECONSTRUCTION OF RICH-CLUB MOTIFS

We report the performance of the method in the setting of a network of 100 nodes having five clusters of 20 nodes each.

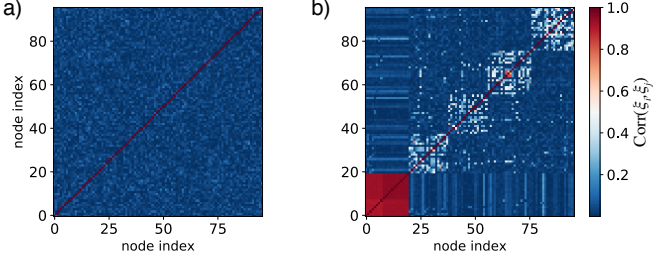


FIG. 5. Reconstruction of a rich-club motif for coupled doubling maps with diffusive coupling $h(x, y) = \sin 2\pi y - \sin 2\pi x$. The left panel is a color map of the pairwise Pearson-correlation between the time-series x_i and x_j . Due to the strong chaotic behaviour this analysis does not give any information on the community structures. In the right panel, we show the colormap of the noise correlation. The clusters are manifested in the correlation structure of the noise, namely, the four communities and the integrating cluster.

Four of these clusters are modeled as Erdős-Renyi random graph with connection probability $p = 0.3$. The remaining cluster is the integrating clusters with connection probability $p = 0.8$. The results are in Figures 5 to 8.

Filtering out the deterministic chaos. We need to filter the contributions of the deterministic parts to reconstruct the community structure. Indeed, for two nodes i and j in the same cluster, the signals have the form

$$x_i(t) = \tilde{X}_i(t) + \zeta(t),$$

and $x_j(t) = \tilde{X}_j(t) + \zeta(t)$ where \tilde{X}_i and \tilde{X}_j is a superposition of the deterministic chaos depending on the variable at the node and independent fluctuations coming from the rest of the network, while ζ is common noise. \tilde{X}_i and \tilde{X}_j have fast decay of correlations, depends on different sets of variables, and for the sake of the following argument, can be assumed to be independent between each other and with ζ . Under these assumptions,

$$\text{Corr}(\tilde{X}_i(t) + \zeta(t), \tilde{X}_j(t) + \zeta(t)) = \frac{\text{Var}(\zeta)}{\sigma_{x_i} \sigma_{x_j}}.$$

Hence, the large values of the variance of the time series leads to strong suppression of the correlation coming from the small common noise ζ .

IV. PREDICTING CRITICAL TRANSITIONS IN RICH-CLUB NETWORKS OF CHAOTIC SYSTEMS

We present another example of how to use the effective network methodology to predict critical transitions. In this case we choose the doubling map for the local dynamics coupled on a rich-club network with clusters sampled as Erdős-Renyi graphs. Consider a rich club network of 2200 elements with 5 clusters. Four of the clusters are made of $N_\ell = 500$ nodes with small degrees, and one cluster (called integrating cluster or rich club) has $N_I = 200$ nodes which are connected with

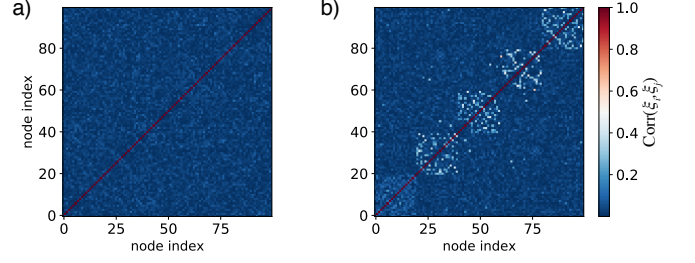


FIG. 6. Reconstruction of rich club for logistic maps with Kuramoto coupling $h(x, y) = \sin 2\pi(y - x)$. The left panel shows a color map of the pairwise Pearson-correlation between the time-series x_i and x_j . In the right panel, we show the colormap of the noise correlation that reveals the community structure and, in particular, the integrating cluster.

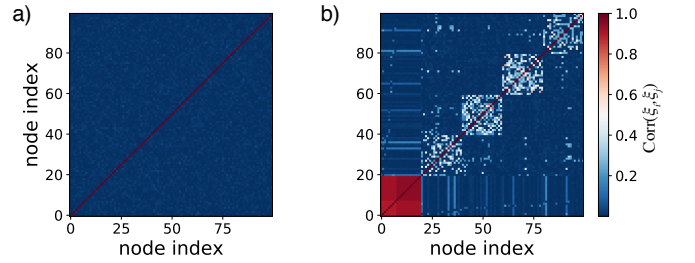


FIG. 7. [Color Online] Reconstruction of rich club for spiking neurons with electrical coupling. The left panel shows a color map of the pairwise Pearson-correlation between the time-series of the membrane potential. The right panel, shows the colormap of the noise correlation revealing the community structure and in particular, the integrating cluster.

most of the network. The edges within a cluster of low degree nodes are assigned above.

As a model for the isolated dynamics, we use the doubling map $f(x) = 2x \bmod 1$ with the diffusive coupling

$$H(x_i, x_j) = h(x_j, x_i) = \varphi(x_j) - \varphi(x_i)$$

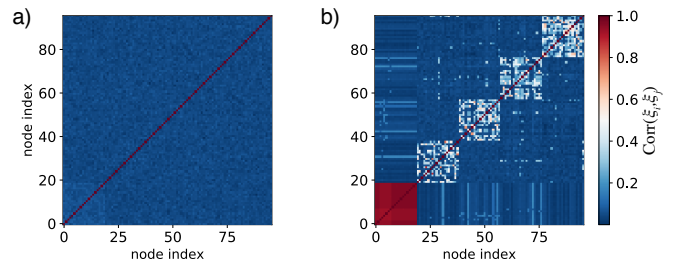


FIG. 8. [Color Online] Reconstruction of rich club for bursting neurons with electrical coupling. The left panel shows a color map of the pairwise Pearson-correlation between the time-series of the membrane potential. The right panel, shows the colormap of the noise correlation revealing the community structure and in particular, the integrating cluster.

where we picked $\varphi(x) = \sin(2\pi x)$. We use the function

$$E(t) = \frac{1}{N_I(N_I - 1)} \sum_{i,j \in IC} \|x_i(t) - x_j(t)\|$$

as an empirical measure of the synchronization level at time t . From a single multivariate time-series, when the coupling is fixed at $\alpha_0 \Delta = 0.2$ (red marker Figure 9), the analysis of $\langle E \rangle$ gives no sign of critical transitions. A statistical analysis shows that the variance of the averaged synchronization error is not amplified, and the extreme value statistics fails to reveal a transition as it also does an analysis of dynamical correlations.

As described above, we can use the effective network methodology to recover the local dynamics f and the effective coupling v . In particular we recover the isolated dynamics $f(x) = 2x$ within 4% accuracy for the poorly connected nodes. The unique physical equilibrium measure for this map is the uniform distribution m on $[0, 1)$. Furthermore, we recover the effective coupling

$$v(x) = \int h(y, x) dm(y) = -\sin 2\pi x.$$

At this point, we know that the approximate evolution of any node i is given by $g_i = f_i + \alpha k_i v_i$, and we can study numerically or analytically this rule to find those values of α for which the integrating cluster exhibits synchrony. The analysis shows that excursions towards synchronization will start once the coupling is increased by 15% (see Figure 9). Below we provide the details on how to recover this critical value of α for which a transition arises.

Reduction in the Integrating Cluster. Nodes in the integrating cluster have roughly degree Δ and make $\kappa \Delta$ connections inside the integrating cluster and $(1 - \kappa) \Delta$ to the rest of the network. The interactions felt by a node in the

rich-club can be split in those coming from nodes in other clusters and those coming from nodes within rich-club itself:

$$\sum_j A_{ij} h(x_i, x_j) = \sum_{j \in RC} A_{ij} h(x_i, x_j) + \sum_{j \notin RC} A_{ij} h(x_i, x_j)$$

But,

$$\sum_{j \notin RC} A_{ij} h(x_i, x_j) = (1 - \kappa) \Delta \int h(x_i, y) d\mu(y) + \xi_i^o(t)$$

where μ is the invariant measure for the nodes outside the integrating cluster¹. Hence, the equation of the integrating cluster can be written as

$$x_i(t+1) = q_i(x_i(t)) + \sum_{j \in RC} A_{ij} h(x_i, x_j) + \xi_i^o(t),$$

where

$$q_i(x_i(t)) = f_i(x_i(t)) + (1 - \kappa) \Delta \alpha \int h(x_i, y) d\mu(y).$$

¹ In the example above μ is the Lebesgue measure m .

We can estimate μ empirically analyzing each cluster. Assuming that

$$h(x, y) = \varphi(y) - \varphi(x),$$

we can recover φ from the analysis of q_i using the reconstruction techniques. In fact, for this particular choice of h , $\int h(x, y) d\mu(y)$ is equal to $-\varphi(x)$ plus a constant. Now if ν is the measure that describes the behaviour of a node in the integrating cluster, then the interaction within the rich-club can be written as

$$\sum_{j \in RC} A_{ij} h(x_i, x_j) = \kappa \Delta \int h(x_i, y) d\nu(y) + \xi^c(t) = \kappa \Delta \left(-\varphi(x) + \int \varphi(s) d\nu(s) \right) + \xi^c(t). \quad (2)$$

Putting the two equations together one has that

$$x_i(t+1) = g_i(x_i(t)) + \alpha \Delta c(\mu, \nu) + \zeta_i(t) \quad (3)$$

where $g_i = f_i - \alpha \Delta \varphi$ models the reduced dynamics and

$$c(\mu, \nu) = (1 - \kappa) \Delta \alpha \int \varphi(s) d\mu(s) + \kappa \Delta \alpha \int \varphi(s) d\nu(s)$$

is the mean contribution from all interactions (inside and outside the integrating cluster). Finally

$$\zeta_i = \xi_i^o(t) + \xi^c(t)$$

combines the effect of the fluctuations.

Model from Data. From a single multivariate time series at a given coupling parameter, shown in Figure 9 as a red dot, we reconstruct the model. First, we obtain the rule g_i which we uncover to be $g_i(x) = 2x - \beta_i \sin 2\pi x \bmod 1$, hence $\beta_i = 0.169$ and this number is nearly independent of the node in the integrating cluster. Hence, we obtain an estimate $(\alpha \Delta)_{\text{est}} = 0.169$. We also obtain that the dynamics of nodes in the communities is well approximated by f .

Next, we need to estimate κ to construct a model for the connectivity of the integrating cluster. From the recovered local dynamics f , one knows that μ is the Lebesgue measure

and, since $\int \varphi d\mu = 0$, we obtain

$$c(\mu, \nu) = \kappa \int \varphi d\nu.$$

In the regime of parameters where the measurements have been made, ν can be obtained empirically and this allows to recover κ since

$$\frac{1}{\int \varphi d\nu} \frac{1}{\alpha \Delta} \langle x_i(t+1) - g_i(x_i(t)) \rangle \rightarrow \kappa, \quad (4)$$

where we evaluate $\int \varphi d\nu$ with respect to the empirically retrieved ν , we substitute $\alpha \Delta$ with the estimated value above,

$$x_i(t+1) = 2x_i(t) - \alpha \Delta \sin(2\pi x_i(t)) + \kappa \Delta \alpha \int \sin(2\pi s) d\nu(s) + \xi(t).$$

When $1/2\pi < \alpha \Delta < 3/2\pi$, the map $2x_i(t) - \alpha \Delta \sin(2\pi x_i(t)) \bmod 1$ has an attracting fixed point at 0. In this new regime, $\nu = \delta_0$ is a self-consistent measure for the integrating cluster, meaning that the measure ν gives rise to an approximated dynamical rule g_i that has ν as equilibrium measure. This can be easily verified since $\int \sin(2\pi s) d\delta_0(s) = 0$. We can then conclude that by selecting a value of the coupling strength such that $\alpha \Delta$ is in the range above, one expects all the states at the nodes in the integrating cluster to evolve towards the point 0 and fluctuate around this point by $\xi(t)$.

To obtain the range of $\alpha \Delta$ such that the fluctuations of E are around twice $\max \|\xi\|$, we notice that since $\nu = \delta_0$ the stability properties are given by the linear stability around $x = 0$. Let u be a small displacement around 0 and let us denote at $J(\alpha) = Dg_i(0)$ the Jacobian of the map g_i at 0. Then we obtain that

$$u(t+1) = \sum_{i=0}^t J(\alpha)^i \xi_i$$

and $\langle \cdot \rangle$ denotes the time average. We obtain that $\kappa = 0.47$. The data analysis reveals that such κ value is nearly independent of the node in the integrating cluster. Moreover, the analysis of the covariance of the noise in the integrating clusters shows a lack of communities and the functional analysis network indicates that the integrating cluster of is a random network 200 nodes with $p = 0.83$. From this analysis, we obtain an estimate for $\Delta \approx p \times 200 / \kappa = 353 = \Delta_{est}$. We are now able to estimate α by $\alpha_{est} = (\alpha \Delta)_{est} / \Delta_{est} = 5 \times 10^{-4}$.

Synchronization Prediction. With the reconstructed data (f, v, A) , we obtain that for a node in the integrating cluster, (3) reads as

and so

$$\|u\| \leq \max \|\xi_i\| / (1 - J(\alpha)),$$

which yields that $1/(1 - J(\alpha)) < 2$. Hence, we obtain $3/4\pi < \alpha \Delta < 5/4\pi$. Because we measured $\alpha \Delta$ as 0.169 in the data given we predict that a high quality coherent state in the rich-club will appear then $\alpha \Delta$ is increased by 40%. This is a agreement with the experiments.

V. CAT CEREBRAL CORTEX

A. Bursting neurons with Chemical Synapsis

We simulated each mesoregion of the cat cerebral cortex network with bursting Rulkov oscillators coupled through chemical synapsis. For such dynamics the parameters are given as $\beta = 4.4$ and $\Delta \alpha = 0.05$ where there is no synchrony between oscillators Fig. 10. We use the simulated data to reconstruct the network structure as shown in Figure 10.

- [1] Brunton, S. L., Proctor, J. L., & Kutz, J. N. Discovering governing equations from data: Sparse identification of nonlinear dynamical systems. *Proc. Natl. Acad. Sci. USA* **113**, 3932–3937 (2015).
- [2] Pereira, T., van Strien, S., & Tanzi, M. *Heterogeneously coupled maps: hub dynamics and emergence across connectivity layers*.

- J. Eur. Math. Soc., preprint: arXiv **1704.06163**, 1–63 (2017)
- [3] de Melo, W., and Van Strien, S., *One-dimensional dynamics*. Springer (2012).
- [4] Rössler, O. E. *An equation for continuous chaos*. Physics Letters A 57, no. 5 (1976): 397–398.

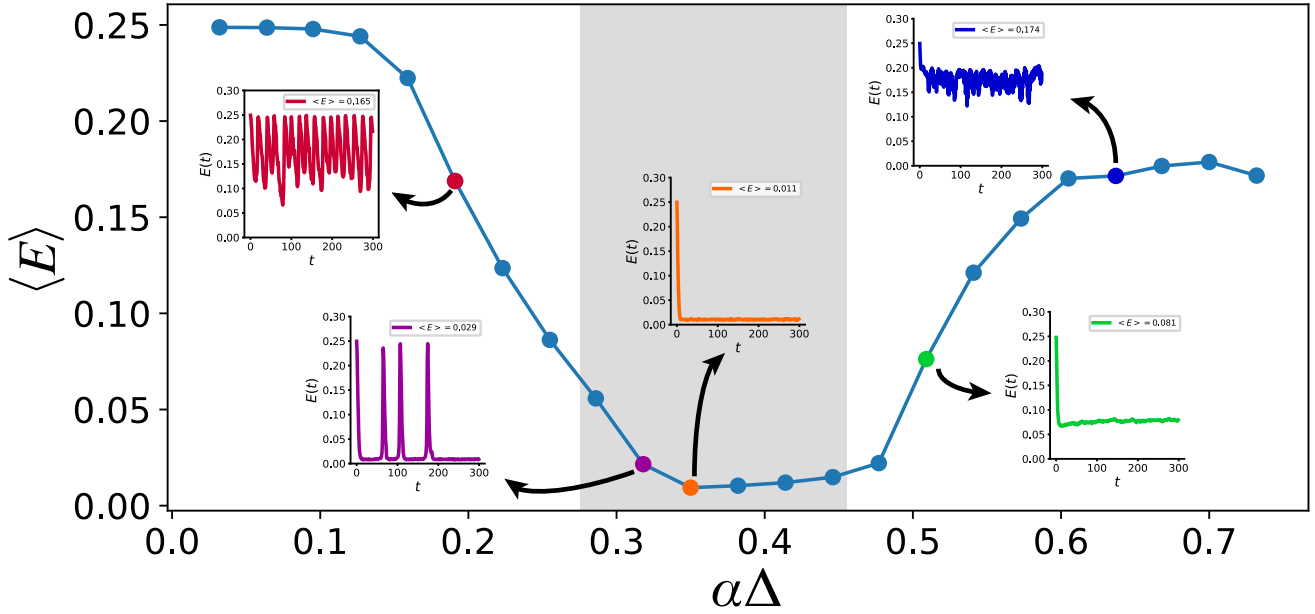


FIG. 9. **Prediction of critical transition in a network with a rich-club motif.** The level of average synchronisation, $\langle E \rangle$ of the integrating cluster is shown for different values of the coupling strength α . Insets show $E(t)$ plotted as a function of time for five points indicated by arrows. For α values in the grey shaded region, $\langle E \rangle$ is close to zero and the integrating cluster exhibits collective behaviour. We can predict the extrema of the shaded region by studying the effective network obtained from a time series without any knowledge of parameters, including $\alpha_0\Delta$. For this prediction, we used the time series when $\alpha_0\Delta = 0.2$ (red point).

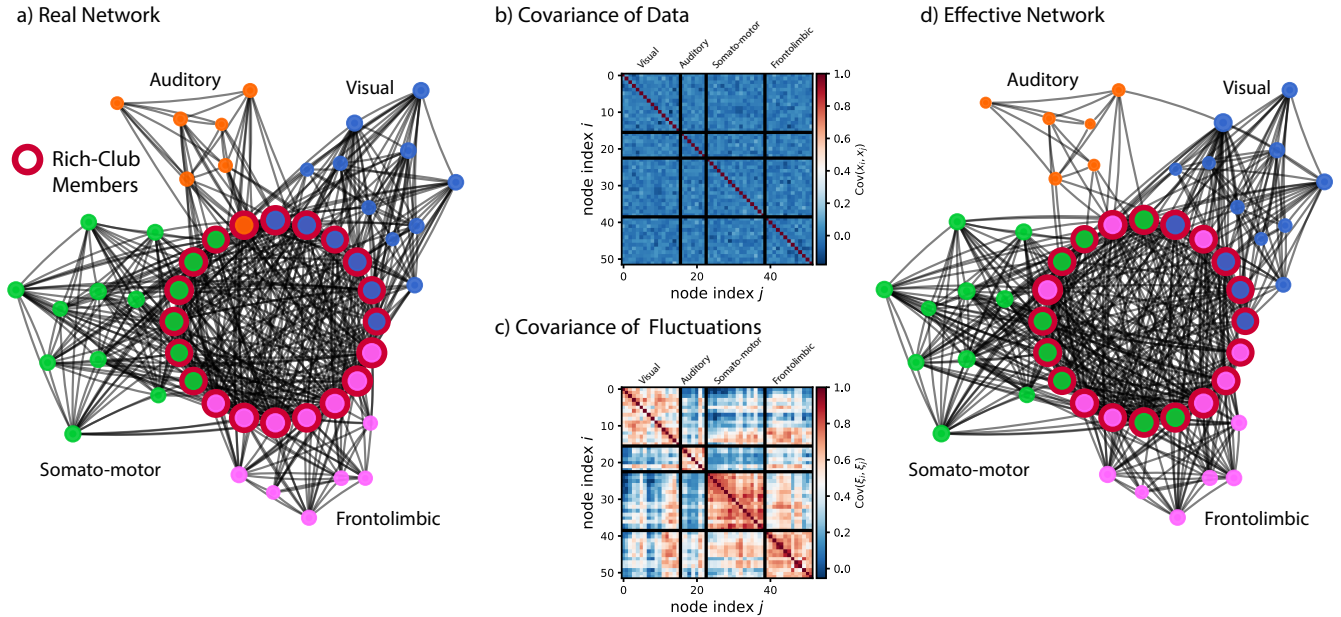


FIG. 10. **Effective network of the cat cerebral cortex.** We use the local dynamics as a spiking neuron coupled via electric synapses with the parameters $\Delta\alpha = 0.05$ and $\beta = 4.4$. (a) The cat cerebral cortex network with nodes colour coded according to the four functional modules. Rich-club members are indicated by red encircled nodes. (b) The covariance matrix of the data cannot detect communities. (c) The covariance matrix of the fluctuations can distinguish clusters of interconnected nodes. (d) A model in the cat cortex constructed via the effective network approach. From the matrix in (c) we can recover a representative effective network. The reconstructed network represents the real network in (a) with good accuracy. See Methods for the details of the detection of communities and rich-club members.